

## Primary Mineralogy of Late Miocene Picrobasalt from Vitim Volcanic Field : Implication to Evolution of Primitive Melts

著者	LITASOV Konstantin, ITO Yoshinori, Malkovets Vladimir, LITASOV Yury, TANIGUCHI Hiromitsu
journal or publication title	Northeast Asian studies
number	7
page range	191-203
year	2003-03-31
URL	<a href="http://hdl.handle.net/10097/41085">http://hdl.handle.net/10097/41085</a>

# Primary Mineralogy of Late Miocene Picobasalt from Vitim Volcanic Field: Implication to Evolution of Primitive Melts

Konstantin LITASOV \*, Yoshinori ITO \*, Vladimir Malkovets \*\*,  
Yury LITASOV \*\*, Hiromitsu TANIGUCHI \*\*\*

**Key words:** picobasalt, mineralogy, olivine, phenocryst, xenolith, crystallization

## Abstract

Primary mineralogy of unique picobasalt from Vitim volcanic field has been described. The picobasalts contain abundant mantle xenoliths. Their amount is up to 50 modal % of the picobasalts. K–Ar estimation of the aphanitic groundmass of the picobasalt indicates the age of 16.3 Ma. This is earliest magmas in the Vitim volcanic field. The picobasalt contains abundant olivine phenocrysts. Modal olivine percentages range from 25 to 42% (of picobasalt minus xenocrysts total). The groundmass composed of clinopyroxene (29% in average), plagioclase (21%), Ti–magnetite (4%), biotite (3%), Cr–spinel (1%), apatite (1.5%), glass (8%) and others (<1.5%). Mg number of olivine phenocrysts ranges from 75 to 82. Calculated Mg number of olivine coexisting with picobasalt is 85–89. This indicates partial disequilibrium, which is probably connected with contamination of the magma by Mg–rich xenolith materials. Interstitial glass from picobasalt groundmass is SiO<sub>2</sub>– and alkali–rich (55–61 wt.% SiO<sub>2</sub>; 3.0–5.1 wt.% Na<sub>2</sub>O and 4.0–4.5 wt.%K<sub>2</sub>O). Crystallization of picobasalt magma was started from olivine and spinel in the middle crust magma chambers (5–8 kbar at 1150–1200°C). Phases of groundmass crystallized under the surface conditions. Crystallization started from clinopyroxene (+minor Ti–magnetite and apatite), following by clinopyroxene + plagioclase, plagioclase only and glass.

---

\* Institute of Mineralogy, Petrology and Economic Geology, Graduate School of Science, Tohoku University

\*\* United Institute of Geology, Geophysics and Mineralogy, Novosibirsk, Russia

\*\*\* Center for Northeast Asian Studies, Tohoku University

## 1. Introduction

Mineralogical studies of mafic and ultramafic volcanic rocks are very important to reconstruct crystallization sequences and magma evolution during ascent to the surface. Ultramafic lavas, picrite, komatiite, meimechite etc. usually contain abundant phenocrysts of earlier generations submerged into the fine-grained groundmass. Many ultramafic volcanics worldwide contain deep-seated xenoliths. In the Baikal rift zone Late Cenozoic basalts containing mantle xenoliths are abundant in the Vitim volcanic field (VF). Mineralogical studies of xenolith-bearing volcanics provide also information on xenolith/host reactions and modification of primary xenolith minerals. In this study we describe primary mineralogy of picobasalt from VF. These picobasalts are well known due to abundant mantle xenoliths, which are described in many papers (Ashchepkov, 1991; Ionov et al., 1993; Glaser et al., 1999; Litasov et al., 2000; Litasov and Taniguchi, 2002).

## 2. Basaltic rocks of the Vitim volcanic field

Geological position of the VF is described by Litasov et al. (1999; 2000) and Litasov and Taniguchi (2002). Within the Vitim field, several volcanic areas were detected. The most of xenolith-bearing volcanics occur within the Bereya area, which is the best studied in terms of chemical composition and age determinations for the volcanics. K–Ar dating indicates at least three eruption stages in the Bereya area (Rasskazov et al., 1996; 2000): (1) Middle Miocene stage (16–14 Ma) manifested by the eruptions of picobasalt and basaltic andesite with subordinate high-Ti olivine tholeiite, (2) Late Miocene stage (8 Ma) is characterized by eruptions of basanite to alkaline olivine basalt and olivine tholeiite, (3) Plio–Pleistocene stage (2–0.8 Ma) is represented by basanite to phonobasanite (Fig.1). The xenolith-bearing picobasalt are unique in the Baikal rift zone. They have Mg# = 62–72 and contain 2.1–3.5 wt.% of Na<sub>2</sub>O + K<sub>2</sub>O (Fig.1).

The picobasalts are complicated for the age determination due to strong alteration and abundant xenogenic material. Ashchepkov (1991) reported age of 26 Ma based on K–Ar data. Recent K–Ar estimation of the aphanitic groundmass indicates the age  $16.3 \pm 1.1$  Ma (Esin et al., 1995). Selected major element data for the picobasalt are presented in Table 1.

## 3. Petrography

The picobasalt contains abundant olivine phenocrysts and overfilled by various xenoliths. Xenolithic material (up to 50 modal % of picobasalt) includes relics of different types of rocks from mantle garnet and spinel peridotite to crustal diorite and granite. Xenocrysts of captured foreign rocks are easily distinguished by similarity of chemical composition with minerals of related xenoliths. Xenocrysts of cumulative rocks as well as megacrysts of clinopyroxene and ilmenite which

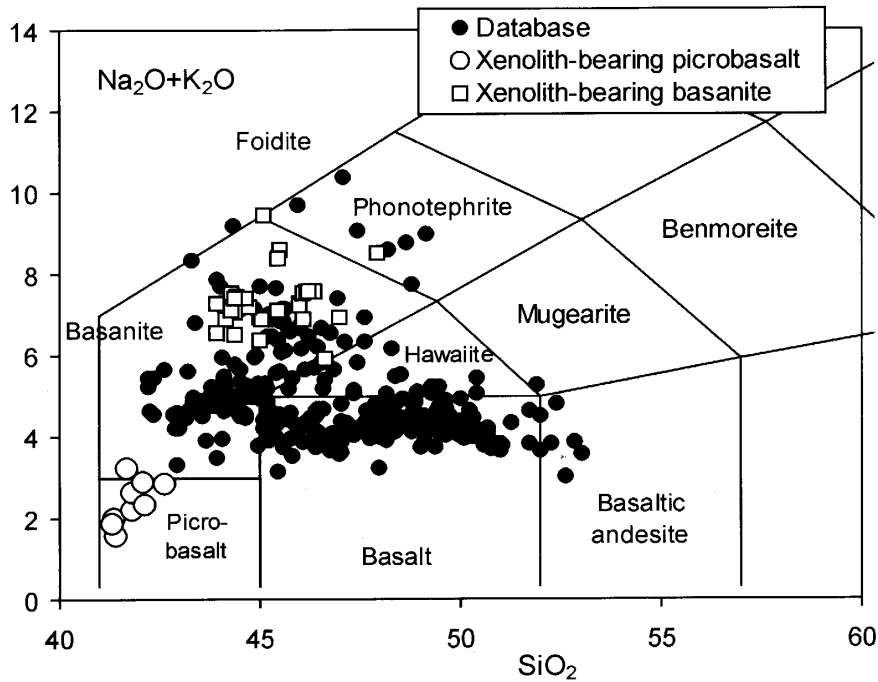


Fig.1. Total alkalis vs. SiO<sub>2</sub> diagrams for the Cenozoic basalts of the Vitim volcanic field. Compiled from Kiselev et al. (1979); Rasskazov (1993); Ashchepkov (1991); Ionov et al. (1993); Esin et al. (1995); Litasov (1996).

**Table 1. Chemical and normative compositions of Miocene picrobasalts from the Vitim volcanic field.**

Sources Sample	[1] 316/1a	[2] C-215	[3] B1-3*	[4] Q	Average of 10	1σ
SiO <sub>2</sub>	41.3	41.8	42.1	42.1	41.9	0.5
TiO <sub>2</sub>	1.88	2.11	2.78	2.30	2.21	0.29
Al <sub>2</sub> O <sub>3</sub>	9.3	9.5	11.2	9.9	9.79	0.64
FeO*	12.3	12.1	12.6	11.9	12.05	0.49
MnO	0.2	0.2	0.2	0.2	0.20	0.02
MgO	16.6	15.5	11.8	14.0	15.3	1.80
CaO	8.9	9.6	10.0	8.8	8.6	0.8
Na <sub>2</sub> O	0.69	0.77	1.66	1.85	1.34	0.60
K <sub>2</sub> O	1.31	1.46	1.24	1.68	1.43	0.31
P <sub>2</sub> O <sub>5</sub>	0.58	0.67	0.78	0.67	0.69	0.09
Total	93.2	93.7	94.2	93.3	93.8	1.6
Mg#	70.6	69.7	62.6	67.8	69.2	3.3
Or	8.2	9.1	7.7	10.5		
Ab	6.2	6.9	12.0	9.3		
An	19.6	19.0	20.2	14.6		
Ne	-	-	1.5	4.0		
Di	18.8	21.5	21.3	21.8		
Hy	3.6	2.0	-	-		
Ol	35.3	32.7	26.8	30.6		
Mt	3.1	3.1	3.2	3.0		
Ilm	3.8	4.2	5.5	4.6		
Ap	1.4	1.6	1.9	1.6		

Sources: 1, Ashchepkov (1991); 2, Esin et al. (1995); 3, Rasskazov et al (1996); 4, Ionov et al (1993). FeO\*, total Fe as FeO. Mg#=100Mg/(Mg+Fe). \*, cleaned from olivine phenocrysts. Normative minerals: Or, orthoclase; Ab, albite; An, anorthite; Ne, nepheline; Di, diopside; Hy, hyperstene; Ol, olivine; Mt, magnetite; Ilm, ilmenite; Ap, apatite.

could be related to picrobasalt host have no significant boundary zoning; whereas minerals of Mg-rich peridotites and other mantle rocks have usually recrystallized aureoles with different compositions (see part 5.2).

Olivine phenocrysts vary in size from 0.1 to 4 mm and are always subhedral to euhedral. Modal olivine percentages range from 25 to 42% (of picrobasalt minus xenocrysts total). The matrix is generally subophitic and composed of elongated clinopyroxene and plagioclase laths (Fig.2). Ti-magnetite and Cr-spinel are typically less than 0.1 mm in size and vary from subhedral crystals to anhedral and rounded forms. Groundmass include also minor amount of biotite laths, apatite, albite, nepheline and Si-rich interstitial glass. Average modal composition of picrobasalt (minus xenocrysts) is calculated as follows: olivine phenocrysts (31%), groundmass of clinopyroxene (29%), plagioclase (21%), Ti-magnetite (4%), biotite (3%), Cr-spinel (1%), apatite (1.5%), glass (8%) and others (<1.5%). Iddingsite is abundant around olivine phenocrysts.

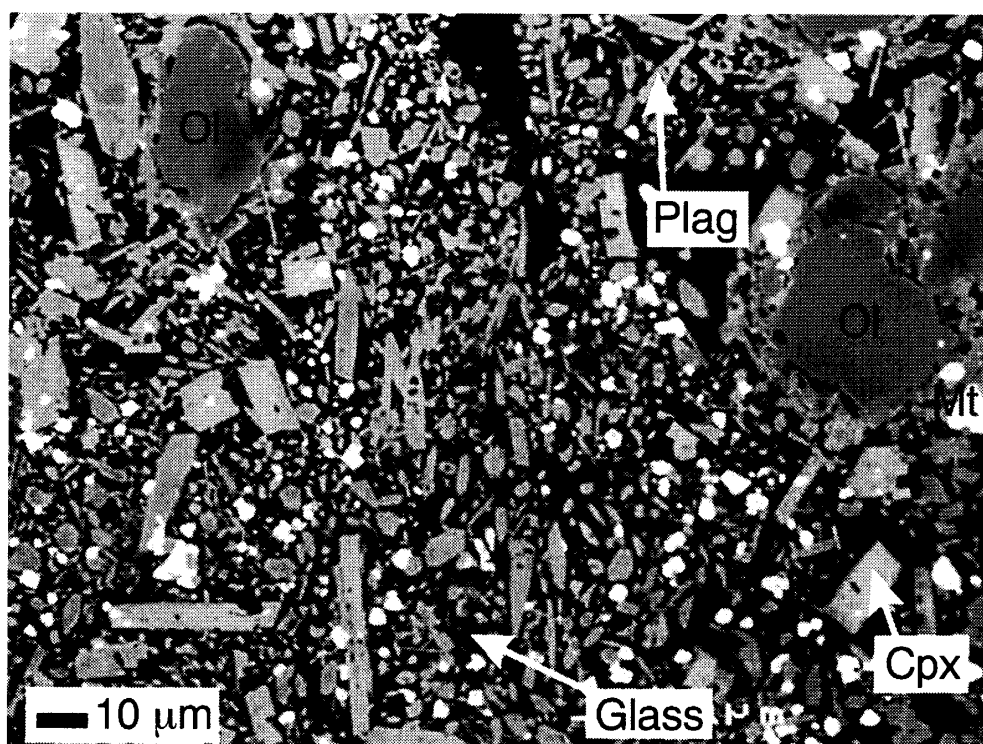


Fig.2. Back-scattered electron image (BEI) of picrobasalt groundmass. Ol, olivine; Cpx, clinopyroxene; Plag, plagioclase; Mt, magnetite.

#### 4. Analytical methods

The igneous mineralogy of picrobasalt was determined on 3 polished thin sections that were selected on the basis of minimum alteration and secondary minerals. The minerals and glasses were analyzed on a JEOL Superprobe (JXA-8800M) microprobe at Institute of Mineralogy, Petrology and Economic Geology, Tohoku University. The standard operating conditions included 15 kV accelerating voltage and 10 nA beam current. Representative analyses of mineral and groundmass glasses

are given in Tables 2 and 3.

## 5. Phase chemistry

### 5.1. Olivine

Composition of olivine phenocrysts is significantly differed from olivine xenocrysts representing disintegrated mantle xenoliths. Mg number of xenolithic olivine range from 88 to 92, whereas Mg number of olivine phenocrysts ranges from 75 to 82. CaO contents of olivine phenocrysts vary widely from 0.16 to 0.65 wt%, remaining high relative to xenolithic olivine (0.05 – 0.09 wt% CaO). NiO contents range in 0.12 – 0.16 wt%. Calculated Mg number of olivine coexisting with microbasalt is 85 – 89 by using  $KD^{Fe-Mg}$  between olivine and melt ( $KD^{Fe-Mg} = (Fe/Mg)_{Ol}/(Fe/Mg)_{melt} = 0.3$  (Roedder and Em-slie, 1970; Ford et al., 1982). These values are higher than Mg number of olivine phenocrysts indicating partial disequilibrium, which is probably connected with contamination of the magma by Mg-rich xenolith materials.

### 5.2. Pyroxenes

Clinopyroxene is a major mineral of groundmass. The clinopyroxene analyses are plotted in the enstatite – diopside – hedenbergite – ferrosilite quadrilateral, following the classification of Morimoto et al. (1988). Majority of groundmass clinopyroxene has Mg number ranged in 67 – 75 and contains  $TiO_2 = 2 - 5$  wt.%,  $Al_2O_3 = 4 - 7$  wt.%,  $Na_2O = 0.3 - 0.6$  wt.% (Fig.3). Clinopyroxene from reactionary rims on the Mg-rich clinopyroxene xenocrysts is similar with groundmass clinopyroxenes (Fig.3). Clinopyroxene in microbasalt is similar with that of some cumulative rocks, like spinel websterites but differed by high  $TiO_2$ .

Scarce grains of Al-rich clinopyroxene and orthopyroxene were detected in microbasalt ground-mass (Table 2), but they may be of hybrid origin.

### 5.3. Spinel and magnetite

Microbasalt contain early-formed Cr-spinels (picotite), which could evolve toward Ti-magnetite during crystallization of microbasalt (Fig.4). In the  $Fe^{3+}/M^{3+}$  total versus  $TiO_2$  diagram spinels from microbasalt are correlated with Fe-Ti-trend observed in many volcanic rocks worldwide (Barnes and Roedder, 2001). This trend can be attributed to evolution of spinel compositions during fractional crystallization of silicate minerals. However, in the  $Fe^{2+}/(Fe^{2+} + Mg)$  versus  $Cr/(Cr + Al)$  spinels from microbasalt show other trend of crystallization with increasing Cr number (Fig.4).

Ti-magnetite of late stage of the microbasalt crystallization contains 15 – 17 wt%  $TiO_2$  and 2 – 5 wt% of  $Al_2O_3$ .

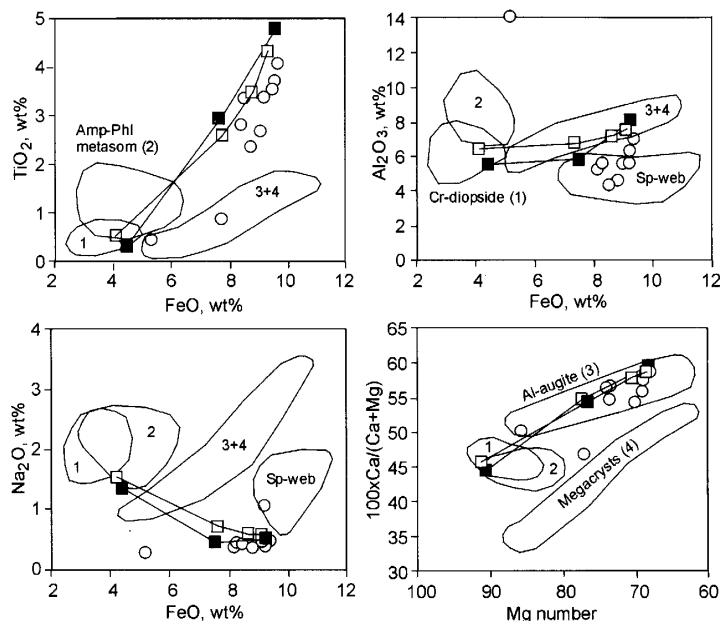


Fig.3. Composition of clinopyroxene from picobasalt groundmass and xenogenic materials. Open circles, clinopyroxene from picobasalts; filled and open squares, herzolitic clinopyroxene with reaction zones of newly formed clinopyroxene related to picobasalt. Fields of clinopyroxene from different types of deep-seated xenoliths are outlined: (1) Cr-diopside, Cr-diopside herzolite and pyroxenite; (2) Amp-Phl-metasom, Amphibole- and phlogopite-bearing metasomatic veins and pyroxenite; (3) Al-augite, Al-augite pyroxenite including group of sp-websterites (Sp-web) with Al- and Na-poor clinopyroxene; (4) Megacrysts, clinopyroxenes of megacryst trend. Data for xenoliths are from Litasov and Taniguchi (2002).

**Table 2. Representative compositions of minerals from Vitim picobasalts.**

Mineral	Ol	Ol	Ol	Ol	Cpx	Cpx	Cpx	Cpx	Cpx	Cpx-c	Cpx-r	Cpx-r	Cpx	Opx
SiO <sub>2</sub>	39.11	38.57	39.02	38.27	49.29	46.35	44.47	43.56	46.42	51.97	45.79	42.09	46.81	50.14
TiO <sub>2</sub>	0.02	0.03	0.06	0.07	0.82	2.67	3.37	4.08	2.83	0.29	3.00	4.82	0.45	0.11
Al <sub>2</sub> O <sub>3</sub>	0.03	0.11	0.03		5.68	4.68	5.66	7.09	5.36	5.57	5.90	8.15	14.46	11.44
Cr <sub>2</sub> O <sub>3</sub>	0.05	0.00	0.07	0.05	0.02	0.04	0.18	-	0.15	1.25	0.31	0.01	0.89	0.97
FeO*	17.58	21.65	18.71	18.13	8.98	8.48	7.80	9.18	7.66	3.00	6.87	9.05	3.92	7.45
MnO	0.21	0.30	0.22	0.22	0.81	0.18	0.06	0.15	0.15	0.11	0.08	0.09	0.38	0.48
MgO	42.05	38.76	43.06	42.38	11.89	13.34	12.20	11.01	12.24	16.54	13.20	10.93	13.24	26.79
CaO	0.43	0.60	0.16	0.19	19.69	22.31	22.16	21.92	22.13	18.56	22.21	22.15	18.67	2.09
NiO	0.15	0.12	0.13	0.14	-	-	-	-	-	-	-	-	-	-
Na <sub>2</sub> O		0.01	0.04	0.01	1.08	0.38	0.45	0.50	0.39	1.35	0.47	0.53	0.30	0.06
Total	99.63	100.16	101.48	99.46	98.25	98.43	96.34	97.49	97.31	98.63	97.82	97.82	99.12	99.52
Mg#	81.0	76.1	80.4	80.6	70.2	73.7	73.6	68.1	74.0	90.8	77.4	68.3	85.7	86.5

Mineral	Mt	Mt	Sp	Sp	Sp	Sp	Sp	Plag	Plag	Ab	Neph	Bt	Bt
SiO <sub>2</sub>	0.08	0.08	0.10	0.10	0.09	0.16	0.18	59.75	53.52	62.97	47.49	34.11	35.88
TiO <sub>2</sub>	15.72	16.94	11.93	6.80	7.23	5.73	3.57	0.03	0.06	0.08	0.05	7.38	6.18
Al <sub>2</sub> O <sub>3</sub>	4.53	2.56	2.40	11.28	8.55	12.75	22.24	24.00	28.33	21.75	29.01	14.98	14.68
Cr <sub>2</sub> O <sub>3</sub>	2.04	0.79	12.89	18.51	16.68	15.67	17.68	0.04	0.04				0.03
Fe <sub>2</sub> O <sub>3</sub>	30.97	31.60	28.01	26.03	25.93	25.79	22.33						
FeO*	42.85	43.66	39.47	32.41	36.13	29.25	22.13	0.64	0.49	0.61	0.83	15.96	15.20
MnO	0.9	0.87	0.96	0.76	0.77	0.77	0.37	0.03			0.06	0.13	0.17
MgO	2.05	1.8	1.18	4.55	1.38	5.09	10.61	0.01	0.01	0.02	0.11	12.00	13.62
CaO	0.1	0.24	0.34	0.31	0.21	0.28	0.13	6.75	11.62	2.63	0.33	0.13	0.19
Na <sub>2</sub> O		0.03		0.08	0.02	0.05	0.03	6.14	4.93	8.81	17.75	0.73	0.73
K <sub>2</sub> O					0.03		0.01	2.03	0.14	1.33	3.86	8.44	8.82
Total	99.24	98.58	97.28	100.83	97.02	95.54	99.28	99.41	99.14	98.19	99.50	93.86	95.50
Mg#												57.3	61.5

Ol, olivine; Cpx, clinopyroxene (c, core and r, rim); Opx, orthopyroxene; Mt, Ti-magnetite; Sp, Cr-spinel (picotite); Plag, plagioclase; Ab, albite; Neph, nepheline; Bt, biotite; See table 1 for other abbreviations. FeO\*, total Fe as FeO, if not specified.

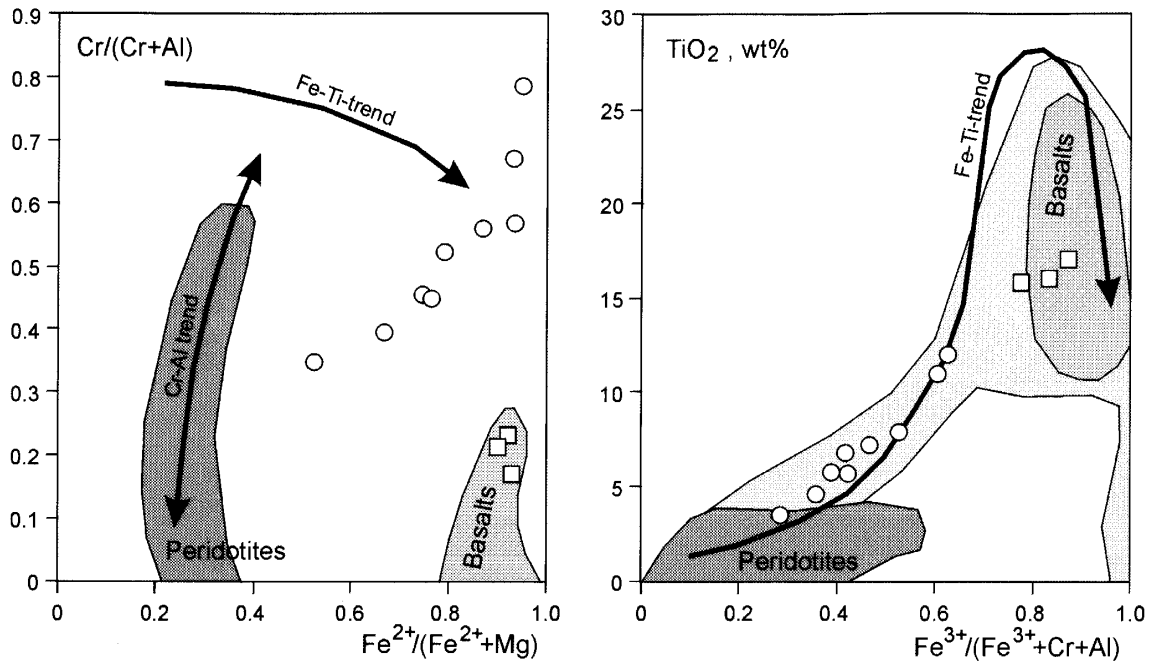


Fig.4. Composition of spinel (circles) and Ti-magnetite (squares) from microbasalt groundmass. Trends of chemical variations in volcanic rocks (Fe-Ti-trend) and in mantle peridotites (Cr-Al-trend) are from Barnes and Roedder (2001). Compositional range of spinel from peridotite xenoliths and spinel from alkaline basalt worldwide after Barnes and Roedder (2001) are also shown. Basaltic contours enclose the most densely packed 50% (small area) and 90% (big and light area in TiO<sub>2</sub> diagram) of the database of Barnes and Roedder (2001).

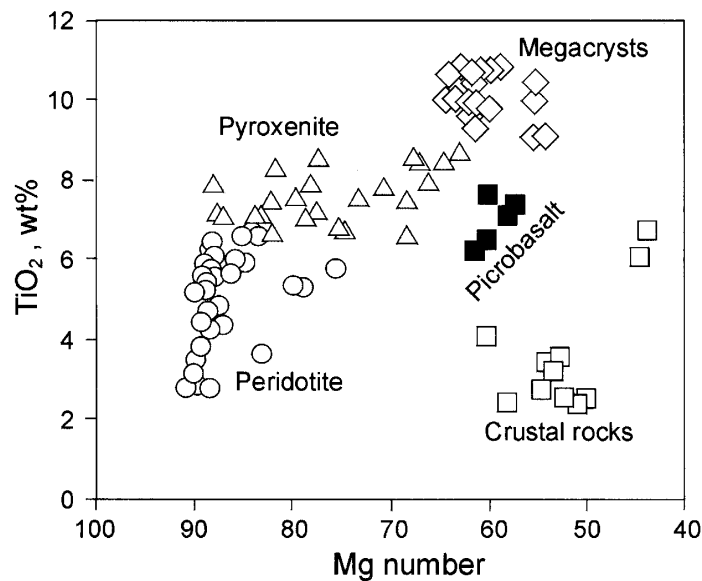


Fig.5. Mg number vs TiO<sub>2</sub> relations in biotite from microbasalt groundmass. Data for peridotites, pyroxenites, megacrysts and crustal rocks are from Litasov and Litasov (1999) and Litasov and Taniguchi (2002).

#### 5.4. Plagioclase

Plagioclase from microbasalts has composition of Ab<sub>70-43</sub>An<sub>30-57</sub>. Rarely pure albite crystals are also detected (Table 2).



### 5.5. Biotite

Formation of biotite during crystallization of picrobasalt is not clear. Composition of biotite laths is not exactly related to any groups of micas from Vitim xenoliths (Fig.5). However, it is possibly related to micas from pyroxenite xenoliths and some crustal rocks. Biotite from picrobasalt has Mg number 56–62 and contains 6–7.5 wt% of  $TiO_2$ .

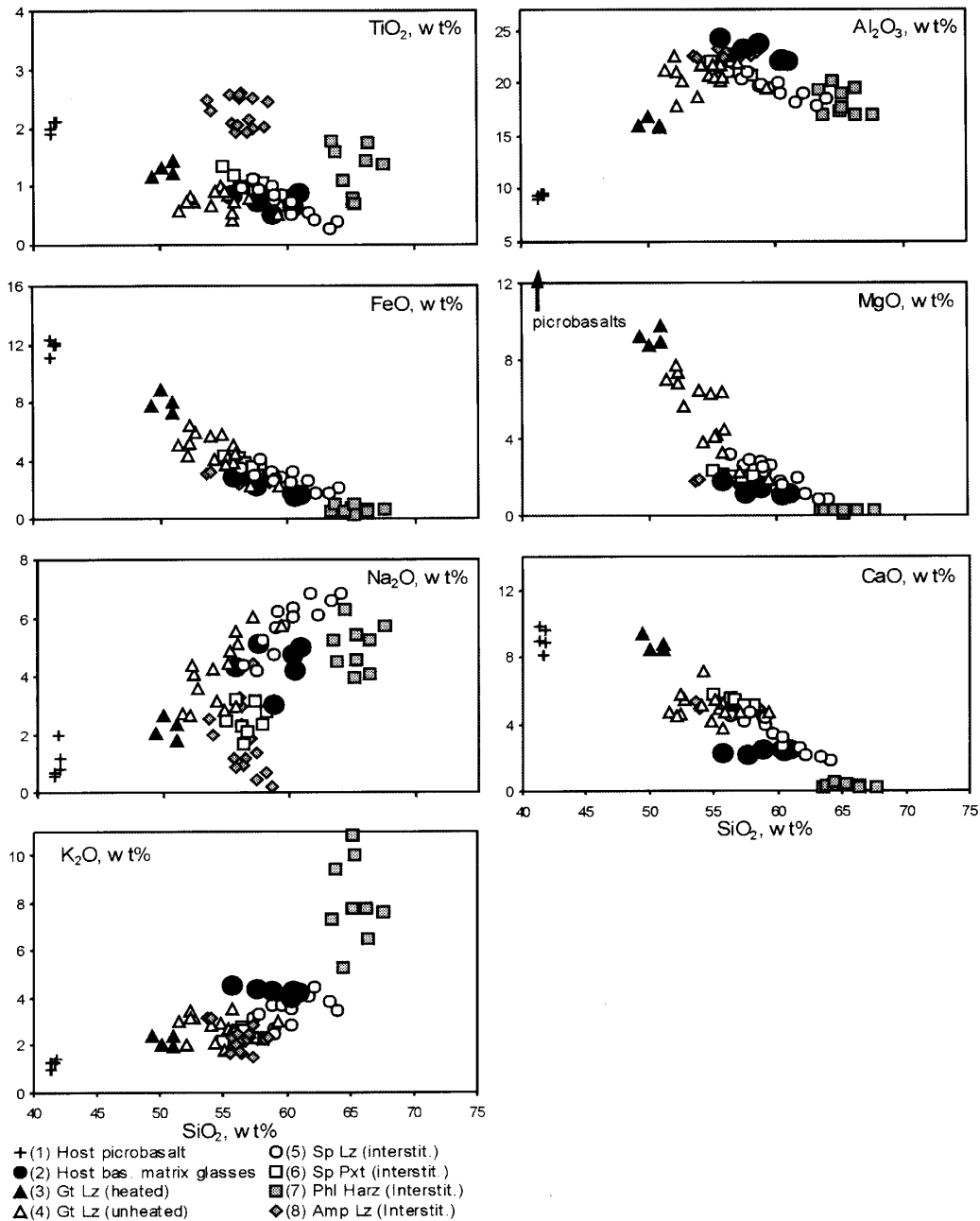


Fig.6. Composition variations vs.  $SiO_2$  content in glasses in the mantle xenolith from the picrobasalts of Picrite Quarry (Vitim volcanic field): (1) host picrobasalt; (2) matrix glass in picrobasalt, (3) heated melt inclusions in garnet lherzolite; (4) unheated melt inclusions in garnet lherzolite; (5) interstitial glass in spinel lherzolite; (6) interstitial glass in spinel pyroxenite; (7) interstitial glass in phlogopite-bearing harzburgite; (8) interstitial glass in amphibole-bearing lherzolite. Data sources: Litasov and Taniguchi (2002), reference therein and our unpublished data.

**Table 3. Representative compositions of groundmass glasses from Vitim microbasalt.**

No	1	2	3	4	5	6	7	8	Ave. of 8	1 $\sigma$
SiO <sub>2</sub>	60.52	60.98	58.82	60.37	55.71	57.63	56.43	58.66	58.64	1.95
TiO <sub>2</sub>	0.65	0.89	0.53	0.79	0.86	0.72	0.65	0.51	0.70	0.14
Al <sub>2</sub> O <sub>3</sub>	22.27	22.09	23.84	22.11	24.33	23.21	22.38	22.89	22.89	0.84
Cr <sub>2</sub> O <sub>3</sub>	–	–	–	0.01	0.01	0.02	0.08	0.02	0.03	0.03
FeO*	1.44	1.66	2.81	1.77	2.83	2.17	2.72	2.42	2.23	0.55
MnO	–	–	0.13	0.01	0.11	0.13	0.05	0.10	0.09	0.05
MgO	1.09	1.15	1.43	1.04	1.75	1.13	0.96	0.72	1.16	0.31
CaO	2.31	2.47	2.44	2.43	2.21	2.11	1.91	0.40	2.03	0.69
Na <sub>2</sub> O	4.21	4.96	3.00	4.73	4.33	5.11	4.40	5.02	4.47	0.69
K <sub>2</sub> O	4.32	4.19	4.30	4.02	4.50	4.37	4.14	4.06	4.24	0.16
P <sub>2</sub> O <sub>5</sub>	0.13	0.40	0.27	0.33	0.34	0.31	0.22	0.21	0.28	0.09
F	0.54	0.03	0.03	0.31	0.55	0.72	–	–	0.36	0.29
Total	97.48	98.82	97.58	97.92	97.53	97.63	93.93	95.00	96.99	1.64
Mg#	57.5	55.3	47.6	51.2	52.4	48.1	38.6	34.7		

See table 1 for other abbreviations.

### 5.6. Glass

Surprisingly, interstitial glass from microbasalt groundmass is SiO<sub>2</sub>–rich (55–61 wt.% SiO<sub>2</sub>) (Table 3). Glass composition is close to alkali feldspar (anorthoclase). Glass has Mg number ranged from 38 to 57 and has high content of Al<sub>2</sub>O<sub>3</sub> (22–24 wt.%) and relatively high alkalis (Na<sub>2</sub>O=3.0–5.1 wt.%; K<sub>2</sub>O=4.0–4.5 wt.%). Glasses from microbasalt plotted close to interstitial glasses in mantle xenoliths (Fig.6). Interstitial xenolith glasses, however, form trends of decrease of SiO<sub>2</sub> with increase CaO, Al<sub>2</sub>O<sub>3</sub> MgO, FeO, TiO<sub>2</sub> and decrease K<sub>2</sub>O and Na<sub>2</sub>O due to reaction with primary xenolith minerals. The microbasalt glasses have no such variations (Fig.6).

## 6. Discussion

Late Miocene microbasalts of the Vitim volcanic field are unique rocks in the Baikal rift zone. Other ultramafic magmas in the volcanic fields of South Baikal, Udokan and Vitim are represented by basanite and nephelinite–leucitite (e.g. Rasskazov, 1993). Primitive composition of the microbasalt suggests generation in deep upper mantle. This is consistent with xenolith sequence observed in the microbasalts. Abundant garnet peridotite xenoliths are unique in Baikal rift system and represent deepest mantle section in the region locating up to 120 km depths (Litasov and Taniguchi, 2002). Eruption energy of the microbasalt was enough to transport huge amount of different xenoliths, probably due to high amount of volatiles, especially CO<sub>2</sub>. Deep–seated xenoliths have size up to 40 cm and their modal abundance in microbasalt can reach 40–50%. Moreover, microbasalts probed all levels and entrained xenoliths of the garnet and spinel facies of the mantle, including cognate cumulates, lower crustal pyroxenites, and middle–upper crustal granite and sedimentary rocks.

Megacryst assemblage of the microbasalt includes clinopyroxene, garnet, ilmenite, biotite, and

related garnet websterites and clinopyroxenites (Litasov et al., 2000; Litasov and Taniguchi, 2002). Late stage cumulates of megacryst assemblage could crystallized from picrobasalt magmas. However, megacrysts are not related to picrobasalt melt transported xenoliths to the surface. The composition of crystallized products suggests high degree of differentiation with total crystallization of megacryst – forming magmas. Detail studies in Vitim field (Litasov et al., 2000) and other regions (Upton et al., 1999; Shaw and Eyzaguirre, 2000) clearly suggest formation of megacryst prior to magmatic episode of xenolith emplacement.

Crystallization of picrobasalt magma was started from olivine and Fe – picotite in the middle crust magma chambers. Olivine phenocrysts are free of primary fluid and melt inclusions. However, pressures of olivine crystallization can be estimated indirectly from pseudosecondary CO<sub>2</sub> – fluid inclusions in xenolith minerals. The density of CO<sub>2</sub> in some inclusions (0.80 – 0.97 g/cm<sup>3</sup>) and homogenization temperature of related melt inclusions (1150 – 1200°C) suggest pressures of 5 – 8 kbar (our unpublished data). Major minerals of groundmass clinopyroxene and plagioclase, as well as restite glass crystallized under the surface conditions. Crystallization started from clinopyroxene (+ minor Ti – magnetite and apatite), following by clinopyroxene + plagioclase, plagioclase only and glass.

Evolution of opaque minerals from Cr – spinel (picotite) to late Ti – magnetite is usual for ultramafic volcanic series (Barnes and Roedder, 2001) but it is not clear for Vitim picrobasalt. We suggest interval between Cr – spinel crystallization in the crystal magma chamber and Ti – magnetite crystallization near the surface, because of differences between Cr/(Cr + Al) and Fe/(Fe + Mg) ratios in spinel and Ti – magnetite (Fig.4).

Crystallization of biotite from picrobasalt melt is ambiguous. Biotite is idiomorphic related to clinopyroxene and plagioclase, suggesting early crystallization (which is impossible) or xenogenic origin. However, mass balance calculations for whole rock indicate 3 – 4 modal % of biotite. Therefore, the question of biotite crystallization should be studied in detail elsewhere.

Occurrence of minor crystals of nepheline, albite, and Al – pyroxenes in the picrobasalt may be connected with local heterogeneity in the crystallizing melt and reaction with fusible xenogenic materials.

## 7. Summary

Primary mineralogy of unique picrobasalt from Vitim volcanic field has been described. The picrobasalts contain abundant mantle xenoliths. Their amount is up to 50 modal % of the picrobasalts. K – Ar estimation of the aphanitic groundmass of the picrobasalt indicates the age of 16.3 Ma. This is earliest magmas in the Vitim volcanic field.

The microbasalt contains abundant olivine phenocrysts. Modal olivine percentages range from 25 to 42% (of microbasalt minus xenocrysts total). The groundmass composed of clinopyroxene (29% in average), plagioclase (21%), Ti-magnetite (4%), biotite (3%), Cr-spinel (1%), apatite (1.5%), glass (8%) and others (<1.5%).

Mg number of olivine phenocrysts ranges from 75 to 82. Calculated Mg number of olivine coexisting with microbasalt is 85–89. These indicate partial disequilibrium, which is probably connected with contamination of the magma by Mg-rich xenolith materials. Interstitial glass from microbasalt groundmass is SiO<sub>2</sub>- and alkali-rich (55–61 wt.% SiO<sub>2</sub>; 3.0–5.1 wt.% Na<sub>2</sub>O and 4.0–4.5 wt.% K<sub>2</sub>O).

Crystallization of microbasalt magma was started from olivine and spinel in the middle crust magma chambers (5–8 kbar at 1150–1200°C). Phases of groundmass crystallized under the surface conditions. Crystallization sequence can be distinguished as follows: clinopyroxene (+ minor Ti-magnetite and apatite), following by clinopyroxene + plagioclase, plagioclase only and glass.

### Acknowledgements

K.L. acknowledges a Center for Northeast Asian Studies (CNEAS), Tohoku University and Japanese Society for Promotion of Sciences for Research Fellowships.

### References

Ashchepkov, I.V., 1991

*Deep-seated xenoliths of the Baikal rift*, Nauka, Novosibirsk (in Russian).

Barnes, S.J. and Roedder, P.L., 2001

The range of spinel compositions in terrestrial mafic and ultramafic rocks, *Jour. Petrol.*, 42, 2279–2302.

Esin, S.V., Ashchepkov, I.V., Ponomarchuk, V.A., Yamamoto, M., Travin, A.V., and Kiselyeva, V.Y., 1995

*Petrogenesis of alkaline basaltoids from the Vitim plateau (Baikal rift zone)*, UIGGM SB RAS Press, Novosibirsk.

Ford, C.E., Russell, D.G., Craven, J.A., and Fisk, M.R., 1982

Olivine-liquid equilibria: temperature, pressure and composition dependence of the crystal/liquid cation partition coefficients for Mg, Fe<sup>2+</sup>, Ca and Mn, *Jour. Petrol.*, 24, 256–265.

Glaser, S.M., Foley, S.F., and Gunter, D., 1999

Trace element enrichment by melt infiltration in garnet- and spinel peridotite xenoliths from

- the Vitim volcanic field, Transbaikalia, eastern Siberia, *Lithos*, 48, 263–285.
- Ionov, D.A., Ashchepkov, I.V., Stosch, H.–G., Witt–Eickschen, G., and Seck, H.A., 1993  
Garnet peridotite xenolith from the Vitim volcanic field, Baikal region: the nature of the garnet–spinel peridotite transition zone in the continental mantle, *Jour. Petrol.*, 34, 1141–1175.
- Kiselev, A.I., Medvedev, M.E., and Golovko, G.A., 1979  
*Volcanism of the Baikal rift zone and problems of deep magma generation*, Nauka, Novosibirsk (in Russian).
- Litasov, K.D., Foley, S.F., and Litasov, Yu.D., 2000  
Magmatic modification and metasomatism of the subcontinental mantle beneath the Vitim volcanic field (East Siberia): evidence from trace element data on pyroxenite and peridotite xenoliths from Miocene picrobasalt, *Lithos*, 54: 83–114.
- , Litasov, Yu.D., Fujimaki, H., Miyamoto T., and Taniguchi H., 1999  
Mantle evolution beneath the Eastern Baikal region, Russia, *Northeast Asian Studies*, 4, 145–172.
- and ----, 1999  
Biotite in megacryst assemblages of the alkaline basaltoids, Vitim plateau, *Geochem. Int.*, 37 (3), 213–223.
- and Taniguchi, H., 2002  
*Mantle evolution beneath the Baikal rift*, CNEAS Monograph Series, 5.
- Litasov, Yu.D., 1996  
Petrology of the mantle–derived xenoliths in alkaline basalts from the Vitim plateau, Trans–Baikal: an approach to model for primitive mantle and metasomatic modification, *Ph.D. Thesis*, Hokkaido Univ.
- Morimoto, N., 1988  
Nomenclature of pyroxenes, *Amer. Mineral.*, 73, 1123–1133.
- Rasskazov, S.V., 1993  
*Magmatism of Baikal rift system*, Nauka, Novosibirsk (in Russian).
- , Ivanov, A.V. and Brandt, S.B., 1996.  
Development of volcanism with rifting relaxation, detail study of Late Cenozoic Bereya area, Vitim volcanic field, *Proc. Geol. Symp. IEC SB RAS*, Irkutsk, Russia, pp.56–58 (in Russian).
- , Logatchev, N.A., Brandt, I.S., Brandt, S.B., Ivanov, A.V., 2000.  
*Geochronology and geodynamics in the Late Cenozoic: (South Siberia – South and East Asia)*, Nauka, Novosibirsk (in Russian).
- Roedder, P.L. and Emslie, R.F., 1970

Olivine-liquid equilibrium, *Contrib. Mineral. Petrol.*, 29, 275-289.

Shaw, C.S.J. and Eyzaguirre, J., 2000

Origin of megacrysts in the mafic alkaline lavas of the West Eifel volcanic field, Germany, *Lithos*, 50, 75-95.

Upton, B.G.J., Hinton, R.W., Aspen, P., Finch, A., Valley, J.W., 1999

Megacrysts and associated xenoliths: evidence for migration of geochemically enriched melts in the upper mantle beneath Scotland, *Jour. Petrol.*, 40, 935-956.